Received May 28, 2018, accepted July 17, 2018, date of publication July 23, 2018, date of current version August 15, 2018.

Digital Object Identifier 10.1109/ACCESS.2018.2858270

Coping Strategy for Multi-Joint Multi-Type Asynchronous Failure of a Space Manipulator

QINGXUAN JIA, XUAN WANG, GANG CHEN, BONAN YUAN, AND YINGZHUO FU
School of Automation, Beijing University of Posts and Telecommunications, Beijing 100876, China

Corresponding author: Gang Chen (buptcg@163.com)

This work was supported by the National Natural Science Foundation of China under Grant 61573066, Grant 61403038, and Grant 61327806.

ABSTRACT To solve the problem that seriously degraded the kinematics performance may not meet the requirements of on-orbit operation tasks, a coping strategy for a multi-joint multi-type asynchronous failure of a space manipulator is proposed in this paper. Based on the entropy method, a comprehensive kinematics performance index (CKPI) is constructed, which can be regarded as the criterion for solving the artificial joint limits and the optimal locked angle of fault joint. And by solving them, a prevention strategy of serious kinematics performance degradation and a treatment strategy of joint free-swinging failure are established. Through synthesizing the above strategies, a coping strategy for a multi-joint multi-type asynchronous failure is constructed. The contributions of this paper are as follows. The constructed CKPI can make the kinematics performances optimal comprehensively in both operation space and joint space of a space manipulator, the method for calculating the artificial joint limits can solve the coupling problem during calculation, and the constructed coping strategy can ensure that the kinematics performance could meet the requirements of on-orbit operation tasks after multi-joint multi-type asynchronous failure. The correctness and effectiveness of the proposed strategy in this paper are verified by a seven-degree-of-freedom space manipulator.

INDEX TERMS Space manipulator, multi-joint failure, coping strategy, artificial joint limit.

I. INTRODUCTION

Space manipulators have been used in space exploration more and more widely, because of whose advantages of large span, high flexibility, strong load capacity, redundant DOF, etc. However, due to the hazardous space environment, heavy operational tasks and complex joint structures, joint failure is likely to occur to a space manipulator during long-term on-orbit service. Especially, the space manipulator applied to the International Space Station is more prone to appear joint failure due to its burdensome tasks, such as spacecraft docking, heavy load carrying and so on [1]. Limited by the hazardous space environment, fault joint usually cannot be repaired promptly. The types of joint failure mainly include locked failure (joint loses motion ability) and free-swinging failure [2] (joint loses active driving force, but keeping the ability of brake control). In practical applications, the possibility of multiple joints failing simultaneously is much lower than joints failing one by one [3], which means that multi-joint asynchronous failure more likely occurs. After multi-joint asynchronous failure occurs, kinematics performances in both joint space and operation space (such as the workspace and the kinematics dexterity) would degrade [4], [5]. In addition, different types of joint failures may occur to the same space manipulator [6]. In order to maximize the application value of a space manipulator, it is necessary to propose a coping strategy for multi-joint multi-type asynchronous failure with kinematics performance of the space manipulator satisfying the requirements of the follow-up on-orbit operation tasks.

On-orbit operation tasks of the space manipulator, which is applied to the International Space Station and its base can be regarded as a fixed one [7], mainly include no-load moving, load carrying, and spacecraft docking [8], [9]. No-load moving tasks have a strict requirement for position and orientation reachability of manipulator's end-effector (kinematics performance in operation space). However, load carrying tasks and spacecraft docking tasks require not only the reachability but also kinematics dexterity (kinematics performance in joint space) to satisfy requirements simultaneously [10]. As a result, the kinematics performances in both operation space and joint space are likely to be required by on-orbit operation tasks. In addition, the accurate evaluation of the kinematics performances of a space manipulator is the key to finish on-orbit operation tasks successfully. Nowadays, there are many indices for evaluating single aspect kinematics performances of space manipulators [11], but almost no CKPI can simultaneously reflect the kinematics performances in both operation space and joint space. Therefore, it is necessary to construct a CKPI.

Aiming at the construction of CKPI, through comprehensively considering local kinematics performance indices such as manipulability, condition number and the minimum singular value, She *et al*. [3] evaluated the comprehensive kinematics performance in joint space. However, the indices are not global ones and the kinematics performances in operation space are not considered in the evaluation process. To solve this problem, Gao and Zhang [12] globalized stiffness, dexterity and manipulability indices, and constructed a CKPI of a space manipulator based on the linear weighting method by synthesizing the above global indices and workspace. However, since all the weights of the sub-indices consisting of the CKPI is equal, the different influence of them on the CKPI cannot be reflected. Thus, through comprehensively considering the average operation time, the average position error, the mean-square deviation of error, and the average operation force, Jin *et al*. [13] constructed a CKPI based on the entropy method. The sub-indices consisting of the CKPI have different weights, but the global fluctuation of manipulator performance in the entire workspace cannot be reflected through the CKPI. In response to this situation, through calculating the global mean value and global fluctuation value of error amplification feature index of condition number, a CKPI that can reflect performance fluctuation was constructed by Ni *et al* [14], but the performance reflected in the CKPI is single. In order to construct a CKPI that cannot only reflect the kinematics performances both in operation space and joint space, but also characterize different influences of the sub-indices exerted on the performance and its fluctuation, the characteristics of the kinematics performances in both operation space and joint space would be analyzed in this paper. We also plan to complete the selection of sub-indices that can comprehensively characterize the kinematics performance of space manipulators. Based on the above analysis and selection, through globalizing the local kinematics performances and calculating the weights of the selected sub-indices, the CKPI can be constructed by the entropy method [15].

Based on the analysis of the characteristics of two aspects kinematics performance indices and the construction of a CKPI, a coping strategy for multi-joint multi-type asynchronous failure can be proposed in accordance with single aspect kinematics performances or the CKPI [16]. After a joint locked failure occurs, the kinematics performance of a space manipulator cannot be optimized by adjusting the locked angle of the fault joint. In addition, the fault joint may be locked at a special angle, which would makes the kinematics performance of the space manipulator degrade seriously (e.g. aiming at a 3-DOF planar series manipulator including 3 equal length links, when the third joint is locked at a special angle with the superposition of links 2 and 3, its workspace will degrade from a circular plane to a circular line [17]). Therefore, in order to prevent serious kinematics performance degradation of a space manipulator, it is necessary to carry out a preventive measure of the degradation before joint locked failure occurs, which means that the artificial limits [18] need to be applied to joints under normal condition, so that the joints will never move to special angles.

For solving the artificial joint limits of space manipulators, some scholars have carried out related studies. In order to give a space manipulator the ability to complete the follow-up on-orbit operation tasks after a single joint locked failure occurs, through calculating self-moving-manifold boundary, a new method for solving the artificial joint limits is proposed by Lewis and Maciejewski [19]. Via releasing artificial limits of healthy joints to corresponding physical limits after joint locked failure, Roberts *et al*. [20] put forward a method to solve the artificial joint limits of a redundant manipulator. To ensure that the volume of the degraded workspace meets the requirements of the follow-up on-orbit operation tasks, Hoover *et al*. [21] completed the calculation of the artificial joint limits based on an analytical method. If the criterion for completing the solution is an index constant (a fixed value of an index) and the artificial joint limits would be released after a joint locked failure occurs, the above studies have a certain reference value for solving the artificial joint limits of space manipulators. In the process of the calculation of artificial joint limits, the criterion for completing the solution usually includes: index constant and index ratio [22] (like the ratio of degraded workspace volume and normal workspace volume). And there are two cases of release and maintain of artificial limits of healthy joints after a joint locked failure occurs. Once the criterion for completing the solution is related to the angle sequence of artificial joint limits, or the artificial limits of healthy joints would be maintained after a joint locked failure occurs, the coupling characteristic will just exist in the solution process [23]. At this time, the expected artificial joint limits cannot be obtained just by the analytical method. In view of this problem, considering the decoupling characteristic of the Newton-Raphson method [24], we plan to use it to solve the artificial joint limits of a space manipulator, so as to construct a prevention strategy of serious kinematics performance degradation of a space manipulator with multi-joint asynchronous locked failure.

After a joint free-swinging failure occurs, the kinematics performance of the space manipulator can be optimized by adjusting the angle of free-swinging joint to the optimal locking angle through underactuated control. Therefore, it is only necessary to take treatment strategy after the failure [25]. The degradation degrees of kinematics performance of a space manipulator could vary by different locked angles of free-swinging fault joint [26], so the optimal locked angle of a free-swinging fault joint needs to be computed to improve the kinematics performance of the fault manipulator. Through analyzing the influence of different locked angles on degradation degrees of workspace, Yang *et al.* [27] obtained the optimal locked angle of a free-swing fault joint of a 3-DOF plane manipulator. Based on the analysis of the joint failure effect on the shape and volume of the degraded workspace, a method for solving the optimal locked angle of a free-swinging fault joint of a redundant manipulator was proposed by Aydin [28]. Through quantifying dexterity, Bergerman and Xu [29] completed the solution of the optimal locked angle of a free-swinging fault joint corresponding to the minimum rate of dexterity degradation of a manipulator. In order to maximize single aspect kinematics performances of a degenerate manipulator, the above methods have completed the solution of the optimal locked angle of a free-swinging fault joint based on different single aspect kinematics performance indices. In this paper, aiming at different requirements of the on-orbit operation tasks, the optimal locked angle of a free-swinging fault joint will be calculated based on different kinematics performances (single aspect kinematics performances or CKPI), and a treatment strategy of joint free-swinging failure of a space manipulator can be constructed.

Based on the above studies, aiming at a space manipulator with joint locked failure, the construction of a prevention strategy of serious kinematics performance degradation can be completed by solving the artificial joint limits. For a space manipulator with joint free-swinging failure, the establishment of the treatment strategy of joint failure can be completed by solving the optimal locked angle of a free-swinging fault joint. Considering that joint locked failure and joint free-swinging failure may asynchronously occur to the same space manipulator, it is almost impossible to determine which type of joint failure would occur firstly [30]. Therefore, none of the above two strategies can be applied to the space manipulator with two types of joint failures. When we cannot determine which type of joint failure would occur firstly, in order to make the kinematics performance of a space manipulator with multi-joint multi-type asynchronous failure meet the requirements of the follow-up on-orbit operation tasks, we will construct a coping strategy for multi-joint multi-type asynchronous failure of a space manipulator through synthesizing the above prevention strategy and treatment strategy.

In summary, aiming at multi-joint multi-type asynchronous failure of a space manipulator applied to the International Space Station, a coping strategy is proposed in this paper. The main contributions of this paper are as follows. Firstly, a method for constructing a CKPI of a space manipulator is proposed, and based on the constructed CKPI, the kinematic performances in both operation space and joint space can be evaluated simultaneously, which can make two aspects kinematic performances achieve a comprehensive optimality. Secondly, aiming at a space manipulator with a joint locked failure, a prevention strategy of serious kinematics performance degradation is proposed; and a treatment strategy of joint free-swinging failure of a space manipulator is developed. Finally, a coping strategy for multi-joint multi-type asynchronous failure of a space manipulator is constructed by synthesizing the above prevention strategy and treatment strategy, which can make the space manipulator meet the requirements of the follow-up on-orbit operation tasks after multi-joint multi-type asynchronous failure. The method proposed in this paper is universal and suitable for the coping process of multi-joint multi-type asynchronous failure of other types of space manipulators.

The rest of this paper is organized as follows: the second chapter carries out the research on constructing a CKPI of a space manipulator; the third chapter proposes a coping strategy for multi-joint multi-type asynchronous failure through synthesizing prevention strategy of serious kinematics performance degradation and treatment strategy of joint free-swinging failure; the fourth chapter carries on simulation to verify the theoretical research; the fifth chapter summarizes the full text.

II. CONSTRUCTION OF CKPI OF A SPACE MANIPULATOR

Kinematics performances of a space manipulator include the ones in operation space and joint space, which affect the efficiency and quality of completion of the on-orbit operation tasks respectively [31]. Considering that most of the on-orbit operation tasks (such as load carrying and Cabin docking) are required for the kinematics performances in both operation space and joint space, a CKPI needs to be constructed to reflect them simultaneously. In this paper, through analyzing the kinematics performance indices in operation space and joint space whose values are related to the locked angle of fault joint, some indices will be selected to synthetically characterize the kinematics performances. Based on entropy method, a CKPI can be constructed by integrating the selected indices, namely sub-indices.

A. ANALYSIS OF KINEMATICS PERFORMANCE INDICES

In order to determine all the sub-indices to constitute a CKPI, the kinematics performances indices in operation space and joint space whose values are related to the locked angle of fault joint need to be analyzed. And they could be determined based on their mathematical expressions and meanings.

In this paper, a n-DOF redundant serial space manipulator is studied in m-dimension operation space, where $m = 6$ and $n > m$. Assume that $J_1, J_2, \ldots, J_n$ represent joints, $q_1, q_2, \ldots, q_n$ represent joint angles, $L_1, L_2, \ldots, L_n$ represent links, and $\Sigma_0, \Sigma_1, \ldots, \Sigma_n$ represent coordinate systems fixed in base and links. Then, the kinematics model of the space manipulator is established as Fig. 1.

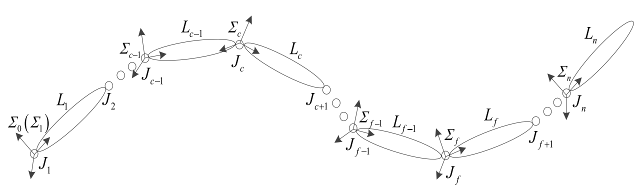

FIGURE 1. Kinematics model of *n*-DOF redundant serial space manipulator

TABLE 1. Kinematics performance indices affected by the locked angle of fault joint in operation space.

	reachable position workspace	partial orientation angle workspace	full orientation angle workspace
expression	$W_{\rm P}=\{P_1, P_2,\ldots, P_N\}$	$W_{\rm OP}=\{P_{\rm OP\_1}, P_{\rm OP\_2},\ldots, P_{{\rm OP}\_N}\}$	$W_{\rm OF}=\{P_{\rm OF\_1}, P_{\rm OF\_2},\ldots, P_{{\rm OF}\_N}\}$
meaning	Reachable position workspace defines the volume $V_{\rm P}$ of the space $W_{\rm P}$ composed of all the reachable position points of end-effector.	Partial orientation angle workspace defines the volume $V_{\rm OP}$ of the space $W_{\rm OP}$ composed of all the reachable position points when end-effector is in any orientation within the partial orientation angle.	Full orientation angle workspace defines the volume $V_{\rm OF}$ of the space $W_{\rm OF}$ composed of all the reachable position points when end-effector is in any orientation within the full orientation angle.
range	$V_{\rm P}\geq 0$	$V_{\rm OP}\geq 0$	$V_{\rm OF}\geq 0$
analysis	The larger the volume $V_{\rm P}$, the higher the position reachability of the manipulator's end-effector.	The larger the volume $V_{\rm OP}$, the higher the partial orientation and position reachability of the manipulator's end-effector.	The larger the volume $V_{\rm OF}$, the higher the full orientation and position reachability of the manipulator's end-effector.

Based on the velocity mapping relationship between operation space and joint space, the velocity transformation relationship of end-effector with respect to joint angles is derived as (1).

$$\boldsymbol{v} = \boldsymbol{J}(\boldsymbol{q})\dot{\boldsymbol{q}} \tag{1}$$

Where Jacobian matrix $\boldsymbol{J}(\boldsymbol{q})$ represents the generalized transmission ratio of joint angle velocity $\dot{\boldsymbol{q}}$ to end-effector velocity $\boldsymbol{v}$. According to singular value decomposition, $\boldsymbol{J}(\boldsymbol{q})$ can be written as

$$\boldsymbol{J}(\boldsymbol{q}) = \boldsymbol{U}\boldsymbol{\Sigma}\boldsymbol{V} \tag{2}$$

Where $\boldsymbol{U}$ represents a $m \times m$ orthogonal matrix and $\boldsymbol{V}$ represents a $n \times n$ orthogonal matrix. The mathematical expression of matrix Σ has following form:

$$\boldsymbol{\Sigma} = \begin{bmatrix} \sigma_1 & 0 & \cdots & 0 & \cdots & 0 \\ 0 & \sigma_2 & \cdots & 0 & \cdots & 0 \\ \vdots & \vdots & \ddots & \vdots & \cdots & \vdots \\ 0 & 0 & \cdots & \sigma_m & \cdots & 0 \end{bmatrix}^{m\times n} \tag{3}$$

Where the diagonal terms $\sigma_1, \sigma_2, \ldots, \sigma_m$ ($\sigma_1 \geq \sigma_2 \geq \ldots \geq \sigma_m \geq 0$) are the singular values of Jacobian matrix $\boldsymbol{J}(\boldsymbol{q})$.

Due to the row ranks of diagonal matrix Σ and Jacobian matrix $\boldsymbol{J}(\boldsymbol{q})$ are equal when the manipulator is in nonsingular configurations, so there is $\text{Rank}(\Sigma) = \text{Rank}(\boldsymbol{J}(\boldsymbol{q})) = m$. When the manipulator is in singular configurations, there is $\text{Rank}(\Sigma) = \text{Rank}(\boldsymbol{J}(\boldsymbol{q})) = r < m$, where the mathematical expression of matrix Σ changes into the following form:

$$\boldsymbol{\Sigma} = \begin{bmatrix} \sigma_1 & 0 & \cdots & 0 & \cdots & 0 & \cdots & 0 \\ 0 & \sigma_2 & \cdots & 0 & \cdots & 0 & \cdots & 0 \\ \vdots & \vdots & \ddots & \vdots & \cdots & \vdots & \cdots & \vdots \\ 0 & 0 & \cdots & \sigma_r & \cdots & 0 & \cdots & 0 \\ \vdots & \vdots & \vdots & \vdots & \ddots & \vdots & \cdots & \vdots \\ 0 & 0 & \cdots & 0 & \cdots & 0 & \cdots & 0 \end{bmatrix}^{m\times n} \tag{4}$$

Where σ_1 and σ_r represent the maximum and minimum nonzero singular value of Jacobian matrix $\boldsymbol{J}(\boldsymbol{q})$, respectively.

Based on the above deduction, we can know that the singular values $\sigma_1, \sigma_2, \ldots, \sigma_m$ (σ_r) of Jacobian matrix $\boldsymbol{J}(\boldsymbol{q})$ can be obtained based on joint angles $q_1, q_2, \ldots, q_n$. Therefore, the values of the kinematics performance indices that are related to the singular values of Jacobian matrix $\boldsymbol{J}(\boldsymbol{q})$ can also be affected by the locked angle of fault joint of a manipulator, such as the mathematical expression of kinematics dexterity index in joint space can be written as

$$D = 1/\min k(\boldsymbol{J}(\boldsymbol{q})) \tag{5}$$

The mathematical expression of reachable position workspace $W_{\rm P}$ in operation space can be written as

$$W_{\rm P} = \left\{ (P_1, P_2, \ldots, P_N) \,\middle|\, P_e = \prod_{i=1}^{n} {}^{i-1}_{\;\;i}\boldsymbol{T}(\boldsymbol{q}),\ e = 1, 2, \ldots, N \right\} \tag{6}$$

Where ${}^{i-1}_{\;\;i}\boldsymbol{T}$ represents the transformation matrix from coordinate system Σ_{i-1} to coordinate system Σ_i.

Through analyzing the relationship between the mathematical expressions and joint angles $q_1, q_2, \ldots, q_n$ or the singular values of Jacobian matrix $\boldsymbol{J}(\boldsymbol{q})$, we can know that the single aspect kinematics performance indices can be affected by the locked angle of fault joint including reachable position workspace $W_{\rm P}$, partial orientation angle workspace $W_{\rm OP}$ and full orientation angle workspace $W_{\rm OF}$ in operation space and the minimum singular value s, condition number k, kinematics dexterity D and manipulability w in joint space. The corresponding mathematical expression, meaning, range and analysis of the above indices are shown in Tables 1 and 2.

B. SELECTION AND TRANSFORMATION OF KINEMATICS PERFORMANCE INDICES

Considering that the characteristics reflected by different kinematics performance indices in operation space and joint space are different [7], therefore, in order to synthetically characterize the kinematics performance in both operation space and joint space, some sub-indices can be selected from the kinematics performance indices that are related to the locked angle of fault joint to construct a CKPI.

Based on Tables 1 and 2, we can know that the number of tasks that can be completed and the speed of planning tasks are influenced by the position and orientation reachability of manipulator's end-effector, which means that the efficiency of completing tasks can be influenced by the reachability.

TABLE 2. Kinematics performance indices affected by the locked angle of fault joint in joint space.

	The minimum singular value	Condition number	Kinematics dexterity	Manipulability
expression	$s = \sigma_r$	$k = \sigma_1 / \sigma_r$	$D = 1/\min k(\boldsymbol{J}(\boldsymbol{q}))$	$w = \sigma_1 \sigma_2 \ldots \sigma_m$
meaning	The minimum singular value defines the distance from singularity.	Condition number defines the dexterity similarity of a manipulator when its end-effector moves to different directions.	Kinematics dexterity defines the dexterity of a manipulator when its end-effector moves to the direction corresponding to the worsts of kinematics performance.	Manipulability defines the comprehensive level of kinematics performance of a manipulator when its end-effector moves to different directions.
range	$s > 0$	$k \in [1,+\infty)$	$D \in (0,1]$	$w \geq 0$
analysis	The larger the minimum singular value s, the less the possibility of singularity.	The closer the k is to 1, the more similar the performances of a manipulator when its end-effector moves to different directions.	The closer the kinematics dexterity D is to 1, the higher the dexterity of a manipulator.	The closer the manipulability w is to 0, the higher the singularity of a manipulator.

In addition, the degrees of running safety and trajectory smoothness can be influenced by the degrees of configuration singularity and isotropy, which means that the quality of completing tasks can be influenced by them [31]. In order to simultaneously improve the efficiency and quality of completing tasks of a space manipulator, it is necessary to maximize the reachability and the configuration isotropy, and minimize the configuration singularity after joint failure occurs.

Through mapping the factors that influence the efficiency and quality of completing tasks of a space manipulator to operation space and joint space, we can know that the position and orientation reachability are the performance in operation space, and the degrees of singularity and isotropy are the performances in joint space. The different kinematics performance indices in operation space or joint space may repeatedly reflect same characteristic of a manipulator [32], such as partial orientation reachability can be characterized by partial orientation angle workspace W_{OP} or full orientation angle workspace W_{OF}, and the kinematics performance corresponding to the worsts direction can be characterized by the minimum singular value s or kinematics dexterity D. In order to reduce the characteristics that are repeatedly reflected in CKPI and improve the efficiency of comprehensive kinematics performance evaluation, we just need to select the part of the kinematics performance indices in both operation space and joint space to construct the CKPI.

Through analyzing the meanings of different kinematics performance indices in Tables 1 and 2, we can know that the position and orientation reachability of manipulator's end-effector can be characterized by reachable position workspace W_{P} and full orientation angle workspace W_{OF}; and that the degree of singularity and isotropy of manipulator configuration can be characterized by the minimum singular value s and condition number k. Therefore, reachable position workspace W_{P}, full orientation angle workspace W_{OF}, the minimum singular value s and condition number k are selected to construct the CKPI.

The CKPI that we will construct is to be used to evaluate the global kinematics performance of a space manipulator. However, the minimum singular value s and condition number k are local kinematics performance indices, so they should be globalized.

Based on Table 2, the expressions of the minimum singular value s and condition number k can be obtained. Through integrating them above reachable position workspace W_{P}, we could get their global levels s_{G} (subscript 'G' means 'global') and k_{G} in the following forms:

$$s_{\mathrm{G}} = \int_{W_{\mathrm{P}}} (s)\, dW_{\mathrm{P}} \tag{7}$$

$$k_{\mathrm{G}} = \int_{W_{\mathrm{P}}} (k)\, dW_{\mathrm{P}} \tag{8}$$

Through dividing s_{G} and k_{G} by the volume of W_{P}, we can obtain the average values of s and k, which are the global minimum singular value $\bar{s}_{\mathrm{G}}$ (superscript '-' means 'average value') and global condition number $\bar{k}_{\mathrm{G}}$. And their mathematical expressions are shown as the following forms:

$$\bar{s}_{\mathrm{G}} = \frac{s_{\mathrm{G}}}{V_{\mathrm{P}}} \tag{9}$$

$$\bar{k}_{\mathrm{G}} = \frac{k_{\mathrm{G}}}{V_{\mathrm{P}}} \tag{10}$$

Where

$$V_{\mathrm{P}} = \int_{W_{\mathrm{P}}} dW_{\mathrm{P}} \tag{11}$$

The overall levels of the values of the minimum singular value and condition number in reachable position workspace can be characterized by the global minimum singular value $\bar{s}_{\mathrm{G}}$ and global condition number $\bar{k}_{\mathrm{G}}$. However, $\bar{s}_{\mathrm{G}}$ and $\bar{k}_{\mathrm{G}}$ cannot characterize the fluctuations of the values of the minimum singular value s and condition number k in the overall reachable position workspace. The smaller the fluctuations, the higher the safety and operation accuracy of a manipulator. Therefore, the influences of the fluctuations need to be considered in the process of constructing the CKPI.

Based on $\bar{s}_G$ and $\bar{k}_G$, the variances D(s) and D(k) above reachable position workspace W_P of s and k can be shown as the following forms:

$$D(s) = \frac{\int_{W_P} (s - \bar{s}_G)^2 \, dW_P}{V_P} \tag{12}$$

$$D(k) = \frac{\int_{W_P} \left(k - \bar{k}_G\right)^2 dW_P}{V_P} \tag{13}$$

Through taking the square root of D(s) and D(k), the standard deviations $\hat{s}_G$ (superscript '∧' means 'fluctuation value') and $\hat{k}_G$ of s and k can be written as the following forms:

$$\hat{s}_G = \sqrt{D(xs)} \tag{14}$$

$$\hat{k}_G = \sqrt{D(k)} \tag{15}$$

Since standard deviation can reflect the volatility of a data set, $\hat{s}_G$ and $\hat{k}_G$ can be used to represent the minimum singular value fluctuation index and the condition number fluctuation index.

To sum up, in order to complete the construction of a CKPI of a space manipulator, it is necessary to synthesize the following 6 sub-indices: reachable position workspace W_P, full orientation angle workspace W_{OF}, the global minimum singular value $\bar{s}_G$, the minimum singular value fluctuation index $\hat{s}_G$, the global condition number $\bar{k}_G$ and condition number fluctuation index $\hat{k}_G$. The above sub-indices all belong to single aspect kinematics performances SI_j of a space manipulator.

C. CONSTRUCTION OF A CKPI BASED ON THE ENTROPY METHOD

In order to characterize the comprehensive kinematics performance in both operation space and joint space of a space manipulator, after the selection and transformation of the kinematics performance sub-indices, the CKPI can be constructed through considering different influences of sub-indices based on the entropy method.

Assuming that a failure occurs to the i^{th} joint J_i of the n-DOF redundant serial space manipulator, and that the fault joint is locked at θ_{i_j} ($j = 1, 2, \ldots, m$), where j represents that fault joint is locked at the j^{th} angle, and m represents the total number of the locked angles of fault joint.

Based on the selected kinematics performance sub-indices, the CKPI can be constructed as (16) based on the entropy method [13].

$$\begin{aligned} CI_j &= \omega_{CI\_1} \times W_P + \omega_{CI\_2} \times W_{OF} + \omega_{CI\_3} \times \bar{s}_G \\ &\quad + \omega_{CI\_4} \times \hat{s}_G + \omega_{CI\_5} \times \bar{k}_G + \omega_{CI\_6} \times \hat{k}_G \\ &= \sum_{h=1}^{6} \left(\omega_{CI\_h} \times P_{j\_h}\right) (j = 1, 2, \ldots, m) \end{aligned} \tag{16}$$

Where, CI_j represents the comprehensive kinematics performance of the manipulator with fault joint locked at θ_{i_j}; ω_{CI_h} represents the weight of the h^{th} sub-index; and P_{j_h} represents the proportion of the h^{th} sub-index value with fault joint locked at θ_{i_j} to the sum of the h^{th} sub-index values with fault joint locked at different angles. Assuming that X_{j_h} is the value of the h^{th} sub-index with fault joint locked at θ_{i_j}, through calculating the proportion of the h^{th} sub-index value with fault joint locked at a certain angle to the sum of the same sub-index values with fault joint locked at different angles, P_{j_h} can be written as

$$P_{j\_h} = \frac{X_{j\_h}}{\sum_{j=1}^{m} X_{j\_h}} \tag{17}$$

Where $h = 1, 2, \ldots, 6$. Based on P_{j_h}, the entropy value e_h of the h^{th} sub-index can be written as

$$e_h = -\frac{\sum_{j=1}^{m} (P_{j\_h} \log(P_{j\_h}))}{\ln(h_{max})} \tag{18}$$

Where $h_{max} = 6$, $0 \leq e_h \leq 1$. Based on e_h, we can get further difference coefficient g_h of the h^{th} sub-index, and g_h can be written as

$$g_h = 1 - e_h \tag{19}$$

Through calculating the proportion of g_h to the sum of the difference coefficients of all the sub-indices, the weight ω_{CI_h} of the h^{th} sub-index can be shown as following form:

$$\omega_{CI\_h} = \frac{g_h}{\sum_{h=1}^{6} g_h} \tag{20}$$

Considering that in the process of constructing a CKPI based on the entropy method [13], the proportion P_{j_h} of the h^{th} sub-index value with fault joint locked at a certain angle to the sum of the same sub-index values with fault joint locked at different angles is adopted. Therefore, there is no influence of dimension, which means that the sub-indices do not need to be standardized. In addition, due to the values of the sub-indices that are all nonnegative, nonnegative treatment for them is not necessary.

Based on the above studies, the construction of CI_j is completed. And the kinematics performances in both operation space and joint space can be reflected simultaneously by the CI_j.

III. COPING STRATEGY FOR MULTI-JOINT MULTI-TYPE ASYNCHRONOUS FAILURE

Due to the hazardous space environment, heavy operational tasks and complex joint structures, multi-joint multi-type failures are likely to occur to space manipulators asynchronously for long-term orbit service. In order to make the kinematics performance (single aspect kinematics performance SI_j or the CKPI CI_j) of the space manipulator meet the requirements of the follow-up on-orbit operation tasks, coping measures should be taken to the multi-joint multi-type asynchronous failures. In this paper, based on the artificial joint limits, a prevention strategy of serious kinematics performance degradation would be proposed for a space manipulator with multi-joint locked failure. Based on the calculation of the optimal locked angle of the fault joint, a treatment strategy of a space manipulator with multi-joint asynchronous free-swinging failures would be developed. On this basis, the coping strategy for multi-joint multi-type asynchronous failure for a space manipulator would be constructed by synthesizing the above two strategies.

A. PREVENTION STRATEGY OF SERIOUS KINEMATICS PERFORMANCE DEGRADATION

Multi-joint asynchronous locked failure is likely to occur to a space manipulator for long-term on-orbit service. In order to make the kinematics performance meet the requirements of the follow-up on-orbit operation tasks after multi-joint locked failure, in this paper, the artificial joint limits would be adopted to a space manipulator under normal condition to avoid moving joints to special angles [16], which could prevent the serious kinematics performance degradation.

1) ANALYSIS OF PREVENTION PROCESS OF SERIOUS KINEMATICS PERFORMANCE DEGRADATION

For a n-DOF redundant serial space manipulator, assuming that $q_i \in [q_i^{\min}, q_i^{\max}]$ $(i = 1, 2, \ldots, n)$ represents the physical joint limits and $\hat{q}_i \in [\hat{q}_i^{\min}, \hat{q}_i^{\max}]$ $(i = 1, 2, \ldots, n)$ represents the artificial joint limits.

For a space manipulator with joint locked failure (or under normal condition), if the DOF of degenerate manipulator $D_f > 6$, in order to prevent serious kinematics performance degradation of the space manipulator after a joint locked failure occurs again, the artificial limits of the healthy joints is still necessary (maintain the artificial joint limits), which leads to the coupling problem in the process of solving artificial joint limits. If $D_f \leq 6$, the kinematics performance degradation of the non-redundant manipulator will be more serious than the redundant one after a joint locked failure occurs again, which may even cause that the space manipulator cannot complete follow-up on-orbit operation tasks [33]. Under this situation, the adoption of artificial joint limits is difficult to prevent serious kinematics performance degradation of the non-redundant serial space manipulator after a joint locked failure occurs again, and may lead to a large decline in the kinematics performance, which cause the manipulator to fail to meet the requirements of the on-orbit operation task. Therefore, when $D_f \leq 6$, the artificial limits will no longer be applied to healthy joints (release the artificial joint limits). The range of each joint angle value of space manipulator is determined by following form:

$$\left[q_i^{\min}, q_i^{\max}\right] = \begin{cases} \left[\hat{q}_i^{\min}, \hat{q}_i^{\max}\right], & D_f > 6 \\ \left[\bar{q}_i^{\min}, \bar{q}_i^{\max}\right], & D_f \leq 6 \end{cases} \tag{21}$$

In order to solve the artificial joint limits of a space manipulator, the criterion for completing the solution also need to be determined. The criterion includes index constant index ratio I_{rat} (subscript 'rat' means 'ratio') and I_{con} (subscript 'con' means 'constant'). For example, when on-orbit operation tasks require the proportion of the volume $\bar{V}$ of degraded workspace to the one $\hat{V}$ of normal workspace is greater than threshold X_{V_rat}, namely that $\bar{V}/\hat{V} \geq X_{V\_\text{rat}}$, where $1 > X_{V\_\text{rat}} > 0$, the criterion for completing the solution can be shown as

$$I_{\text{rat}} = \bar{V}/\hat{V} \geq X_{V\_\text{rat}} \tag{22}$$

Since the solution of $\hat{V}$ is related to the artificial joint limits $\hat{q}_i \in [\hat{q}_i^{\min}, \hat{q}_i^{\max}]$ $(i = 1, 2, \ldots, n)$, therefore, when the criterion for completing the solution is I_{rat}, the coupling problem will appear in the process of calculating artificial joint limits.

When on-orbit operation tasks require $\bar{V} \geq V_{\text{con}}$, where V_{con} is a constant and $\hat{V} > V_{\text{con}} > 0$, the criterion for completing the solution can be shown as

$$I_{\text{con}} = \bar{V} \geq V_{\text{con}} \tag{23}$$

Note that the selection of the criterion depends on the on-orbit operation tasks.

After judging whether the artificial joint limits are released and selecting the criterion for completing the solution, through judging whether the coupling problem is in the process of calculation, the method for solving the artificial joint limits of a space manipulator can be determined as Table 3.

TABLE 3. Selection of the methods to solve the artificial joint limits.

	Release the artificial joint limits	Maintain the artificial joint limits
I_{rat}	Newton-Raphson method	Newton-Raphson method
I_{con}	Analytical method or Newton-Raphson method	Newton-Raphson method

The analytical method shown in Table 3 has already existed, based on which the artificial joint limits can be solved by single calculation. However, the analytical method is only suitable under the condition that the criterion for completing the solution is an index constant and the artificial joint limits would be released after joint failure. Therefore, a method of solving the artificial joint limits based on the Newton-Raphson method is proposed in this paper.

2) SOLUTION OF THE ARTIFICIAL JOINT LIMITS BASED ON THE NEWTON-RAPHSON METHOD

From Table 3, we can know that the Newton-Raphson method has a universal application. Its characteristic is that the artificial joint limits of a space manipulator can be solved through iterative calculation in all cases. And the specific process for solving the artificial joint limits of the space manipulator can be shown as followings.

Step 1: Let $K = 0$ (K represents the iterative number for solving artificial joint limits based on the Newton- Raphson method), assume that the artificial limits of all joints outside J_c of the manipulator are taken as the corresponding physical limits, shown as (24), and turn to Step 2.

$$\left[\hat{q}_i^{\min}, \hat{q}_i^{\max}\right] = \left[\bar{q}_i^{\min}, \bar{q}_i^{\max}\right] \tag{24}$$

Where $i = 1, 2, \ldots, c-1, c+1, \ldots, n$.

Step 2: Assume that q_{c_j} is the locked angle of J_c, let q_{c_j} traverse the rotation range $[q_c^{\min}, q_c^{\max}]$ of J_c at interval of Δq, then the number m of q_{c_j} can be shown as

$$m = \left\lceil (q_c^{\max} - q_c^{\min})/\Delta q \right\rceil \tag{25}$$

Where, $\lceil \cdot \rceil$ is the rounding-up operation, which can make the number m as an integer. And Δq can be determined based on the actual calculation amount. According to the mathematical expression of kinematics performance (SI_j or CI_j), calculate the kinematics performance values I_j with J_c locking at different angles. Construct set $\boldsymbol{I}$ that contains all the kinematics performance values I_j, shown as (26), and turn to Step 3.

$$\boldsymbol{I} = \left\{ I_j | I_j = \mathrm{XI}(q_{c\_j}), (j = 1, 2, \ldots, m) \right\} \tag{26}$$

Where XI represents SI_j or CI_j.

Step 3: Based on set $\boldsymbol{I}$, determine the angle ranges $[q_{c_\mu}, q_{c_\mu}](\mu = 1, 2, \ldots)$ of J_c with satisfying $I_j \geq I_{\mathrm{desired}}$, where I_{desired} represents index threshold value (such as index constant I_{con} or index ratio I_{rat}) required by follow-up on-orbit operation tasks of the space manipulator with joint failure. Based on (27), select the maximum angle range $[\hat{q}_c^{\min}, \hat{q}_c^{\max}]$ from $[q_{c\_\mu}, q_{c\_\mu}]$ as the artificial limit of J_c, and turn to Step 4.

$$\left[\hat{q}_c^{\min}, \hat{q}_c^{\max} \right] = \mathrm{Max} \left\{ [q_{c\_\mu}, q_{c\_\mu}], (\mu = 1, 2, \ldots) \right\} \tag{27}$$

Step 4: Repeat the procedures from Step 1 to Step 3 to solve the artificial limits $\hat{q}_i \in [\hat{q}_i^{\min}, \hat{q}_i^{\max}]$ $(i = 1, 2, \ldots, c-1, c+1, \ldots, n)$ of all joints outside J_c, and complete the single calculation of artificial joint limits $\hat{q}_i \in [\hat{q}_i^{\min}, \hat{q}_i^{\max}](i = 1, 2, \ldots, n)$ of the space manipulator, let $K = K + 1$ and turn to Step 5.

Step 5: If $K = 1$, or $1 < K < K_{\max}$ ($K_{\max}$ is the upper limit of the iterative number) but the error of the upper and lower limits of the artificial joint limits obtained from two adjacent times cannot meet (28), based on $\hat{q}_i \in [\hat{q}_i^{\min}, \hat{q}_i^{\max}]$ $(i = 1, 2, \ldots, n)$, repeat the procedures from Step 1 to Step 4 to solve the artificial joint limits of the space manipulator again. If $1 < K < K_{\max}$ and the error meets (28), decoupling is completed. Output the artificial joint limits $\hat{q}_{i(K)} \in [\hat{q}_{i(K)}^{\min}, \hat{q}_{i(K)}^{\max}]$ $(i = 1, 2, \ldots, n)$ solved at the K^{th} time and finish the solution of the artificial joint limits. If $K = K_{\max}$ but the error cannot meets (28), revise the threshold values and repeat the procedures from Step 1 to Step 5 until that $1 < K < K_{\max}$ and the error meets (28).

$$\begin{cases} (\hat{q}_{i(K-1)}^{\max} - \hat{q}_{i(K)}^{\max}) \leq \upsilon \\ (\hat{q}_{i(K-1)}^{\min} - \hat{q}_{i(K)}^{\min}) \leq \upsilon \end{cases} \tag{28}$$

Where, υ represents the maximum permissible error, which can be determined according to the total amount of iteration computation and the required accuracy of artificial joint limits.

Based on the above process, the artificial joint limits $\hat{q}_i \in [\hat{q}_i^{\min}, \hat{q}_i^{\max}]$ $(i = 1, 2, \ldots, n)$ of a space manipulator can be solved by using the Newton-Raphson method, which can solve the coupling problem in the process of calculation and has a universal application. The specific process for solving the artificial joint limits based on the analytical method is Step 1 to Step 4 in the above process. If the criterion for completing the solution is not related to the artificial joint limits and the artificial joint limits would be released after joint failure, the artificial joint limits of the space manipulator can be solved by single calculation only based on the analytical method.

3) CONSTRUCTION OF PREVENTION STRATEGY OF SERIOUS KINEMATICS PERFORMANCE DEGRADATION

For a n-DOF redundant serial space manipulator, firstly, based on Table 3, select a method to solve the artificial joint limits $\hat{q}_i \in [\hat{q}_i^{\min}, \hat{q}_i^{\max}]$ $(i = 1, 2, \ldots, n)$. Then, limit the rotation ranges of all the joints to the solved artificial limits under normal condition. When J_c locked failure occurs, if the space manipulator whose DOF has degraded is still a redundant one (i.e. $\mathrm{D}_f > 6$), the artificial limits of healthy joints $J_1, J_2, \ldots, J_{c-1}, J_{c-2}, \ldots, J_n$ of the degraded manipulator need to be solved, and so on, until the space manipulator is a non-redundant one. At this time, the artificial limits of all the healthy joints should be released to the corresponding physical limits, that means $q_i \in [\bar{q}_i^{\min}, \bar{q}_i^{\max}]$ $(i = 1, 2, \ldots, c-1, c+1, \ldots, n)$, so that the kinematics performance of the degraded space manipulator meets the requirements of the on-orbit operation tasks.

Based on the above strategy, the prevention of serious kinematics performance degradation of a space manipulator can be realized. The constructed prevention strategy can ensure that the kinematics performance of a space manipulator still meets the requirements of the follow-up on-orbit operation tasks after multi-joint locked failure.

B. TREATMENT STRATEGY OF JOINT FREE-SWINGING FAILURE

In order to make the kinematics performance (SI_j or CI_j) of a space manipulator be qualified for the follow-up on-orbit operation tasks after joint free-swinging failure occurs, treatment measure should be taken to the failure. For a n-DOF redundant serial space manipulator, it is usually necessary to lock the fault joint when the f^{th} joint J_f (subscript 'f' means 'free-swinging' and the possible value of f is $1, 2, \ldots, n$) has a free-swinging failure. Considering that the kinematics performance of a space manipulator varies with the locked angles of fault joint, in order to make kinematics performance I_j of the space manipulator can still meet the requirements $I_j \geq I_{\mathrm{desired}}$ of the follow-up on-orbit operation tasks after joint free-swinging failure occurs, in this paper, the values of kinematics performance I_j would be solved when fault joint is locked at different angles. The locked angle q_{f_desired} corresponding to the maximum kinematics performance value would be selected as the optimal locked angle of a free-swinging fault joint, and the treatment of joint failure also can be completed by locking fault joint at the optimal locked angle. By this analogy, the treatment of multi-joint free-swinging failure of a space manipulator can be accomplished.

Assume that the swing range of J_f is $q_f \in [q_f^{\min}, q_f^{\max}]$ when J_f has a free-swinging failure. Let q_f traverse the swing range at interval of Δq, then based on (25), m locked angles of free-swinging fault joint J_f can be obtained. And Δq can be determined based on the actual calculation amount. According to m, we can obtain a set $\boldsymbol{q}_f$ of locked angles of fault joint J_f, and the expression of set $\boldsymbol{q}_f$ is as following form:

$$\boldsymbol{q}_f = \left\{ q_{f\_j} | q_{f\_j} = q_f^{\min} + j \times \Delta q \right\} (j = 1, 2, \ldots, m) \quad (29)$$

According to the mathematical expression of kinematics performance, calculate the kinematics performance values I_j when joint J_f is locked at different angles. All the kinematics performance values can make up the set $\boldsymbol{I}$. Through corresponding the different locked angles in set $\boldsymbol{q}_f$ to the different kinematics performance values in set $\boldsymbol{I}$, two dimensional array set $\boldsymbol{Q}$ made up of the locked angles and the corresponding kinematics performance values can be obtained, and set $\boldsymbol{Q}$ can be expressed as

$$\boldsymbol{Q} = \left\{ \left(q_{f\_1}, I_1\right), \left(q_{f\_2}, I_2\right), \ldots, \left(q_{f\_m}, I_m\right) \right\} \in \boldsymbol{R}^{2\times m} \quad (30)$$

Where $\boldsymbol{R}^{2\times m}$ represents a $2 \times m$ Euclidean space. The maximum kinematics performance value $I_j^{\max}$ in set $\boldsymbol{I}$ can be obtained based on the following equation:

$$I_j^{\max} = \mathrm{Max}\{\boldsymbol{I}\} \quad (31)$$

Through comparing the solved maximum kinematics performance values $I_j^{\max}$ to the values in set $\boldsymbol{Q}$, we can obtain the same one ($I_{\max\_only}$) or some kinematics performance values ($I_{\max\_1}, I_{\max\_2}, \ldots, I_{\max\_x}$) as $I_j^{\max}$. Judging: if the kinematics performance value is unique, select the locked angle q_{f_only} in set $\boldsymbol{Q}$ corresponding to $I_{\max\_only}$ as the optimal locked angle $q_{f\_desired}$ of fault joint. If $I_{\max\_1}$, $I_{\max\_2}, \ldots, I_{\max\_x}$ equal $I_j^{\max}$, select the x locked angles $q_{f\_\max\_1}, q_{f\_\max\_2}, \ldots, q_{f\_\max\_x}$, in set $\boldsymbol{Q}$ corresponding to $I_{\max\_1}, I_{\max\_2}, \ldots, I_{\max\_x}$. Considering the required time and energy for adjusting free-swinging fault joint simultaneously, the angle $q_{f\_desired}$ that is the closest to the shutdown angle q_{f_stop} of fault joint can be selected from the x locked angles based on following equation:

$$q_{f\_desired} = \mathrm{Min}\left\{ q_{f\_desired\_i} \left| \left(q_{f\_desired\_i} = \left| q_{f\_\max\_i} - q_{f\_stop} \right| \right) \right. \right\} \quad (32)$$

Where, $i = 1, 2, \ldots, x$, and q_{f_stop} represents the angle of fault joint J_f after the manipulator stops. Based on above process, the optimal locked angle $q_{f\_desired}$ of fault joint J_f can be obtained. Through controlling healthy joints based on the underactuated control method [32], the fault joint can be adjusted to the optimal locked angle and be locked. By this analogy, the treatment of multi-joint free-swinging failure of a space manipulator can be completed.

In summary, through solving the optimal locked angle of fault joint and locking it after each joint free-swinging failure, a treatment strategy of multi-joint free-swinging failure can be constructed. The constructed treatment strategy can ensure that the kinematics performance of a space manipulator meets the requirements of the follow-up on-orbit operation tasks after multi-joint asynchronous free-swinging failure.

C. COPING STRATEGY FOR MULTI-JOINT MULTI-TYPE ASYNCHRONOUS FAILURE

The various types of joint failure may occur to the same space manipulator. In order to ensure that the kinematics performance of a space manipulator meets the requirements of the follow-up on-orbit operation tasks after multi-joint multi-type asynchronous failure, it is necessary to construct a coping strategy. The constructed prevention strategy of serious kinematics performance degradation and treatment strategy of multi-joint asynchronous free-swinging failure can make the kinematics performance of a space manipulator with multi-joint asynchronous locked or free-swinging failure meet the requirements of the follow-up on-orbit operation tasks. However, they are not enough for multi-joint multi-type asynchronous failure. Therefore, the two strategies above for different types of joint failures are applied to the same space manipulator to cope with the multi-joint multi-type asynchronous failure. And the coping strategy for multi-joint multi-type asynchronous failure is constructed in Fig. 2.

If joint locked and free-swinging failures asynchronously occur to the same n-DOF redundant serial space manipulator, considering that it is almost impossible to determine which type of joint failure would occur firstly before joint failure [30], and that the DOF of a normal space manipulator is usually greater than 6, in order to prevent serious kinematics performance degradation caused by joint locked failure occurring firstly, the artificial limits of joints $J_1, J_2, \ldots, J_n$ need to be applied to a normal space manipulator, i.e.

$$\left[q_i^{\min}, q_i^{\max} \right] = \left[\hat{q}_i^{\min}, \hat{q}_i^{\max} \right], \quad (i = 1, 2, \ldots, n) \quad (33)$$

After a joint locked failure is handled in a space manipulator, considering that DOF D_f of degenerate manipulator affects the continuous use of prevention strategy of serious kinematics performance degradation, therefore, it is necessary to judge D_f after each joint failure treatment. If $\mathrm{D}_f > 6$, the artificial joint limits $\hat{q}_i \in [\hat{q}_i^{\min}, \hat{q}_i^{\max}]$ $(i = 1, 2, \ldots, n)$ would continue to be applied to prevent serious kinematics performance degradation. If $\mathrm{D}_f \leq 6$, the artificial joint limits would be released, which means that the prevention strategy of serious kinematics performance degradation would be no longer used, i.e.

$$\left[q_i^{\min}, q_i^{\max} \right] = \left[\bar{q}_i^{\min}, \bar{q}_i^{\max} \right], \quad (i = 1, 2, \ldots, c-1, c+1, \ldots, n) \quad (34)$$

After joint free-swinging failure occurs to a space manipulator, the fault joint J_f would usually be locked at the optimal locked angle $q_{f\_desired}$. Due to the locked angle of fault joint can be changed after joint free-swinging failure occurs, it is unnecessary to consider whether the DOF of the degraded space manipulator is redundant. As long as the space manipulator is in the working state, the joint free-swinging failure can

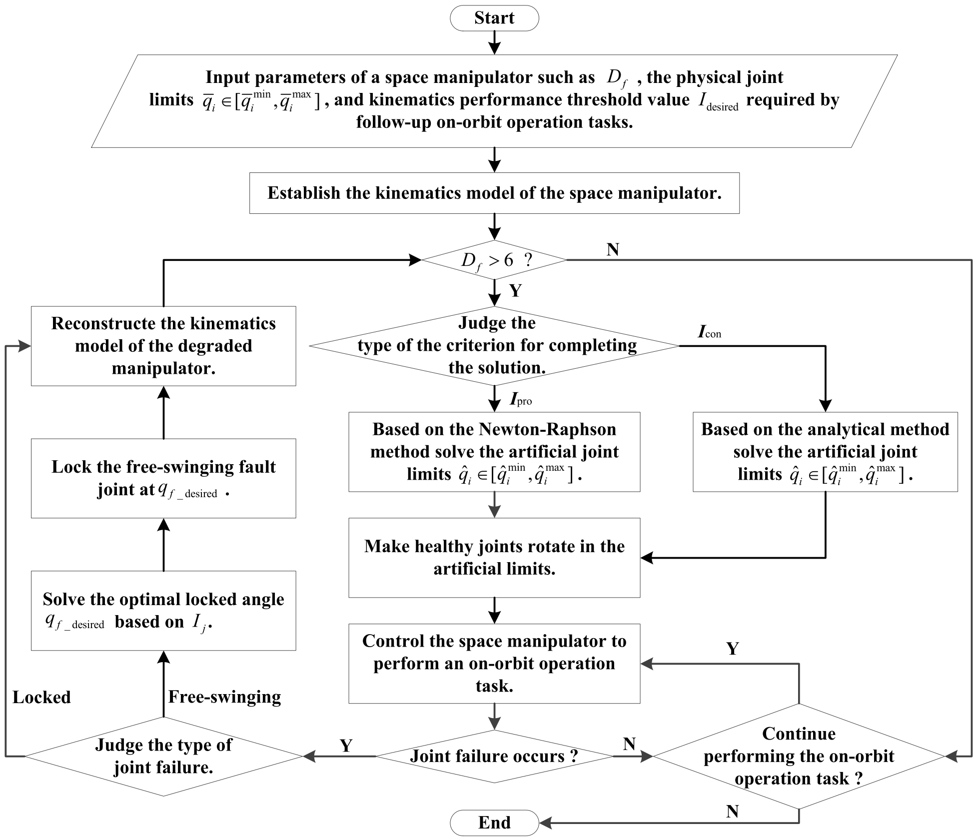

FIGURE 2. Coping strategy for multi-joint multi-type asynchronous failure.

be solved by locking the fault joint J_f at the optimal locked angle $q_{f\_desired}$.

Based on the constructed coping strategy above, the kinematics performance of a space manipulator with multi-joint multi-type asynchronous failure can still meet the requirements of the follow-up on-orbit operation tasks, so that the engineering application value of the space manipulator can be maximized during the entire service cycle.

IV. SIMULATION

In this paper, a 7-DOF space manipulator that is applied to the International Space Station, shown in Fig. 3, is regarded as the research object for simulation. Its DH parameters are shown in Table 4.

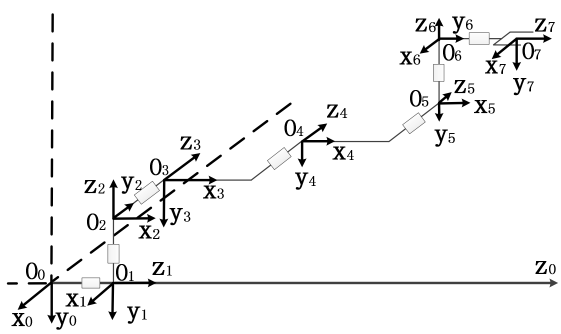

FIGURE 3. Kinematics model of the 7-DOF manipulator.

TABLE 4. DH parameters of the 7-DOF manipulator.

Link i	θ_i(°)	d_i(m)	a_i(m)	α_i(°)
0	\	\	0	0
1	0	0.6	0	90
2	90	0.5	0	-90
3	0	0.5	5	0
4	0	0.5	5	0
5	0	0.5	0	90
6	-90	0.5	0	-90
7	0	0.6	\	\

A. SOLUTION OF THE ARTIFICIAL JOINT LIMITS OF THE MANIPULATOR

Considering that it is almost impossible to determine which type of joint failure would firstly occur, therefore, in order to prevent serious kinematics performance degradation caused by joint locked failure occurring firstly,

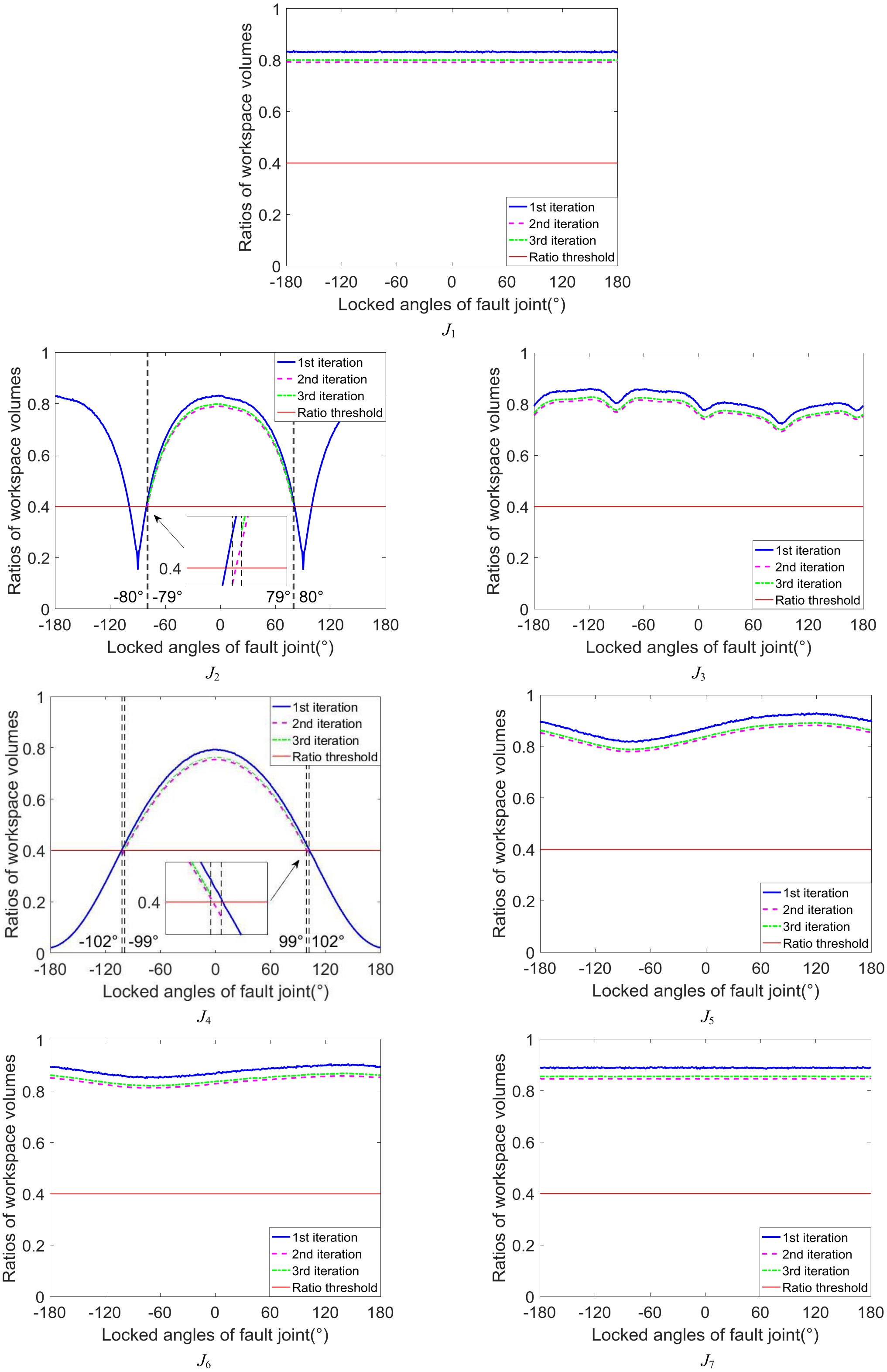

FIGURE 4. Release the artificial limits of healthy joints and satisfy $\bar{V}/\hat{V} \geq 40\%$.

the artificial joint limits need to be applied to a normal manipulator.

Let $\bar{V}$ represent the volume of workspace of the degraded manipulator and $\hat{V}$ represent the volume of workspace of the normal manipulator with the artificial limits being applied to joints. Through generating $N = 200000$ workspace points based on the Monte Carlo method, the volume $\hat{V}$ can be obtained and $\bar{V}$ of the degraded workspace of the manipulator

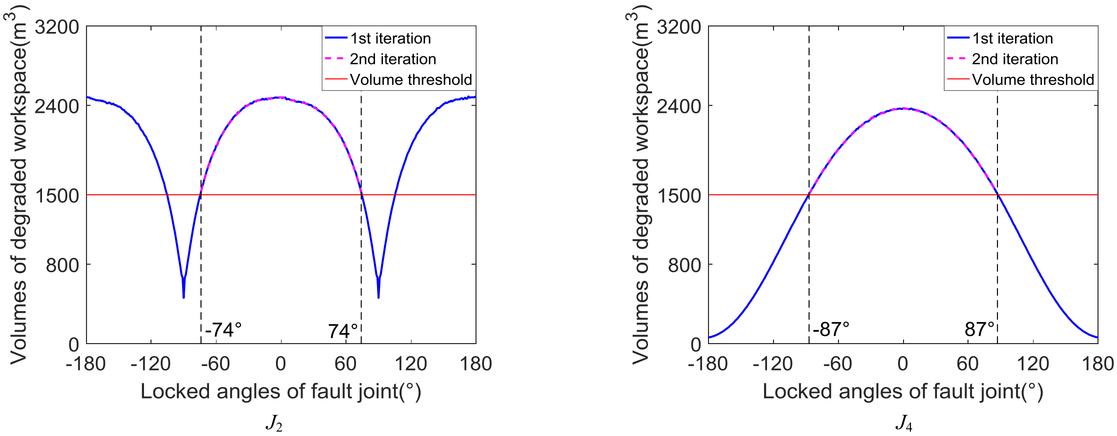

FIGURE 5. Release the artificial limits of healthy joints and satisfy $\bar{V} \geq 1500m^3$.

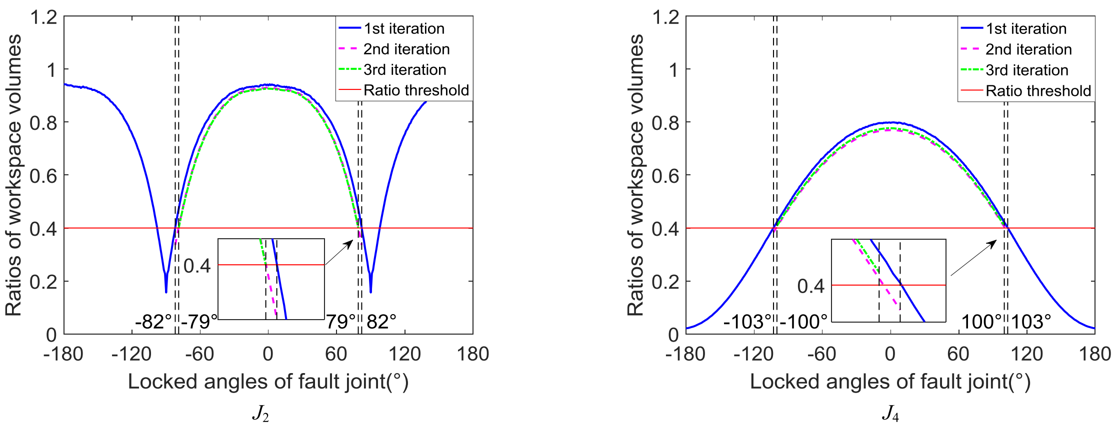

FIGURE 6. Maintain the artificial limits of healthy joints and satisfy $\bar{V}/\hat{V} \geq 40\%$.

can be solved with each joint locked at different angles. The angles can be obtained by traversing the rotation range of each joint with interval $\Delta q = 1°$. Considering the size of the total amount of iteration computation and the required accuracy of artificial joint limits simultaneously, determine the error $\upsilon \leq 1°$ of the upper and lower limits of the artificial joint limits obtained from two adjacent times.

1) RELEASE ARTIFICIAL JOINT LIMITS AND REGARD INDEX RATIO AS CRITERION FOR COMPLETING THE SOLUTION

When the artificial limits of healthy joints are released after joint locked failure, and on-orbit operation tasks require $\bar{V}/\hat{V} \geq 40\%$ (index ratio), regard $\bar{V}/\hat{V} \geq 40\%$ as the criterion for completing the solution. Solve the artificial joint limits based on the Newton-Raphson method, and the artificial limits of J_1 to J_7 of the manipulator are $[-180° \sim 180°]$, $[-79° \sim 79°]$, $[-180° \sim 180°]$, $[-99° \sim 99°]$, $[-180° \sim 180°]$, $[-180° \sim 180°]$, $[-180° \sim 180°]$. The solution curves are given in Fig. 4.

2) RELEASE ARTIFICIAL JOINT LIMITS AND REGARD INDEX CONSTANT AS CRITERION FOR COMPLETING THE SOLUTION

When the artificial limits of healthy joints are released after joint locked failure, and $\bar{V} \geq 1500m^3$ (index constant) is the criterion for completing the solution, the artificial joint limits of the manipulator are solved by the analytical method, and the result of the artificial limits of J_1 to J_7 are $[-180° \sim 180°]$, $[-74° \sim 74°]$, $[-180° \sim 180°]$, $[-87° \sim 87°]$, $[-180° \sim 180°]$, $[-180° \sim 180°]$, $[-180° \sim 180°]$. In view of the length limitation of this paper, the solution curves of artificial limits of only J_2 and J_4 are given in Fig. 5.

3) MAINTAIN ARTIFICIAL JOINT LIMITS AND REGARD INDEX RATIO AS CRITERION FOR COMPLETING THE SOLUTION

When the artificial limits of healthy joints are maintained after joint locked failure, and $\bar{V}/\hat{V} \geq 40\%$ is the criterion for completing the solution, the artificial joint limits of the manipulator needs to be solved by the Newton-Raphson method, and the result of the artificial limits of J_1 to J_7 are $[-180° \sim 180°]$, $[-79° \sim 79°]$, $[-180° \sim 180°]$, $[-100° \sim 100°]$, $[-180° \sim 180°]$, $[-180° \sim 180°]$, $[-180° \sim 180°]$. The solution curves of the artificial limits of J_2 and J_4 are given in Fig. 6.

4) MAINTAIN ARTIFICIAL JOINT LIMITS AND REGARD INDEX CONSTANT AS CRITERION FOR COMPLETING THE SOLUTION

When the artificial limits of healthy joints are maintained after joint locked failure, and $\bar{V} \geq 1500m^3$ is the criterion

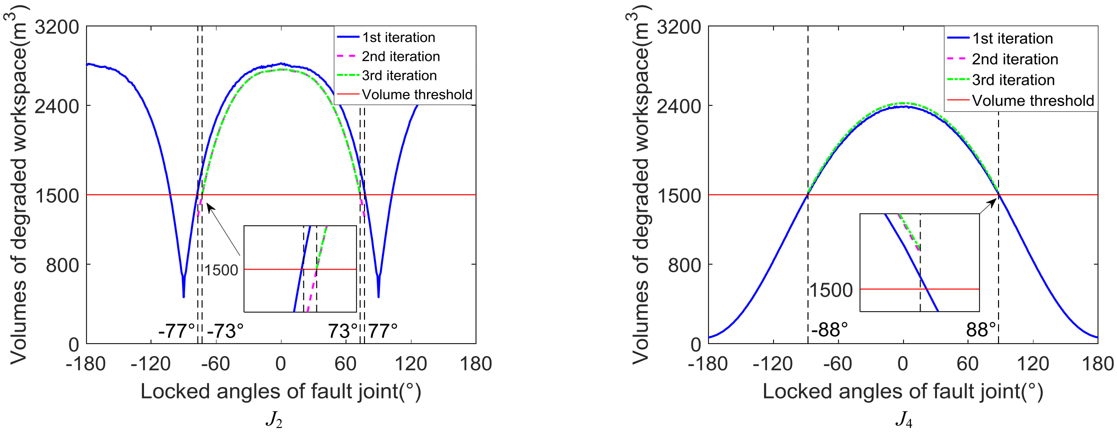

FIGURE 7. Maintain the artificial limits of healthy joints and satisfy $\bar{V} \geq 1500\text{m}^3$.

for completing the solution, the artificial joint limits of the manipulator needs to be solved still by the Newton-Raphson method in this paper. The result of the artificial limits of J_1 to J_7 are $[-180° \sim 180°]$, $[-73° \sim 73°]$, $[-180° \sim 180°]$, $[-88° \sim 88°]$, $[-180° \sim 180°]$, $[-180° \sim 180°]$, $[-180° \sim 180°]$. The solution curves of the artificial limits of J_2 and J_4 are given in Fig. 7.

Based on the above solution, it is shown that just when the artificial limits of healthy joints would be released after joint locked failure, and the criterion for completing the solution is an index constant (such as $\bar{V} \geq 1500\text{m}^3$), the artificial joint limits of the manipulator can be solved by the analytical method. In other cases, the artificial joint limits need to be solved by the Newton-Raphson method. This conclusion is completely corresponding to Table 3. Therefore, the correctness and universality of the proposed method for solving the artificial joint limits of a space manipulator in this paper can be proved.

B. COPING WITH MULTI-JOINT MULTI-TYPE ASYNCHRONOUS FAILURE OF THE MANIPULATOR

Assume that the kinematics performance of the 7-DOF space manipulator in both operation space and joint space should be no less than the corresponding threshold required by an on-orbit operation task. Calculate the single aspect kinematics performances of the space manipulator under different conditions of joint locked failure, and select the failure conditions where the single aspect kinematics performances meet the requirements. Based on (16) - (20), solve the minimum CKPI of the space manipulator under the selected failure conditions. Then, the threshold of the CKPI CI_j (required by the on-orbit operation task) can be determined.

Assume that the CKPI threshold of the 7-DOF manipulator required by an on-orbit operation task is $\text{CI}_j \geq 0.006$. Considering that the artificial limits of healthy joints would be released after joint locked failure, let $\upsilon = 1°$, and set the initial artificial joint limits as the corresponding physical joint limits $q_i \in [q_i^{\min}, q_i^{\max}] = [-180°, 180°]$, $(i = 1, 2, \ldots, 7)$. Through generating N = 200000 workspace points based on the Monte Carlo method, the CKPI values of the manipulator with each joint locked at different angles, which are obtained by traversing the rotation range of each joint with interval $q = 3°$, are solved. Judge whether the CKPI values meet the criterion for completing the solution, and solve the artificial joint limits of the manipulator based on the analytical method. The solution curves of the artificial joint limits are shown in Fig. 8. The corresponding artificial joint limits of J_1 to J_7 are $[-180° \sim 180°]$, $[-165° \sim -15°]$, $[-180° \sim 180°]$, $[-171° \sim 171°]$, $[-171° \sim 171°]$, $[-159° \sim -21°]$, $[-180° \sim 180°]$.

Assume that J_2 locked failure occurs firstly, even if J_2 locked at $-15°$, which corresponds to the minimum CKPI value of the manipulator, the CKPI value is $\text{CI}_j = 0.0161 > 0.006$, and it meets the requirements of the on-orbit operation task. If the artificial joint limits are not applied, the CKPI of the manipulator may be severely degraded to $\text{CI}_j = 0.0025 < 0.006$ after J_2 locked failure occurs, which means that the kinematics performance of the manipulator cannot meet the requirement of the on-orbit operation task.

After J_2 locked failure, the artificial limits of healthy joints of the manipulator are released to the corresponding physical limits. Assume that the free-swinging failure of J_6 occurs in the following process of completing the on-orbit operation task. Then, the optimal locked angle of J_6 can be solved based on the treatment strategy of joint free-swinging failure proposed in this paper, and the solution result is shown as Fig. 9. Furthermore, we can know that the optimal locked angle of J_6 is $\pm 90°$. And when J_6 is locked at $\pm 90°$, the CKPI value of the manipulator is $\text{CI}_j = 0.0067 > 0.006$, which means that the kinematics performance of the degraded manipulator still meets the requirement of the on-orbit operation task. Therefore, the correctness and effectiveness of the coping strategy for multi-joint multi-type asynchronous failure of a space manipulator proposed in this paper are verified.

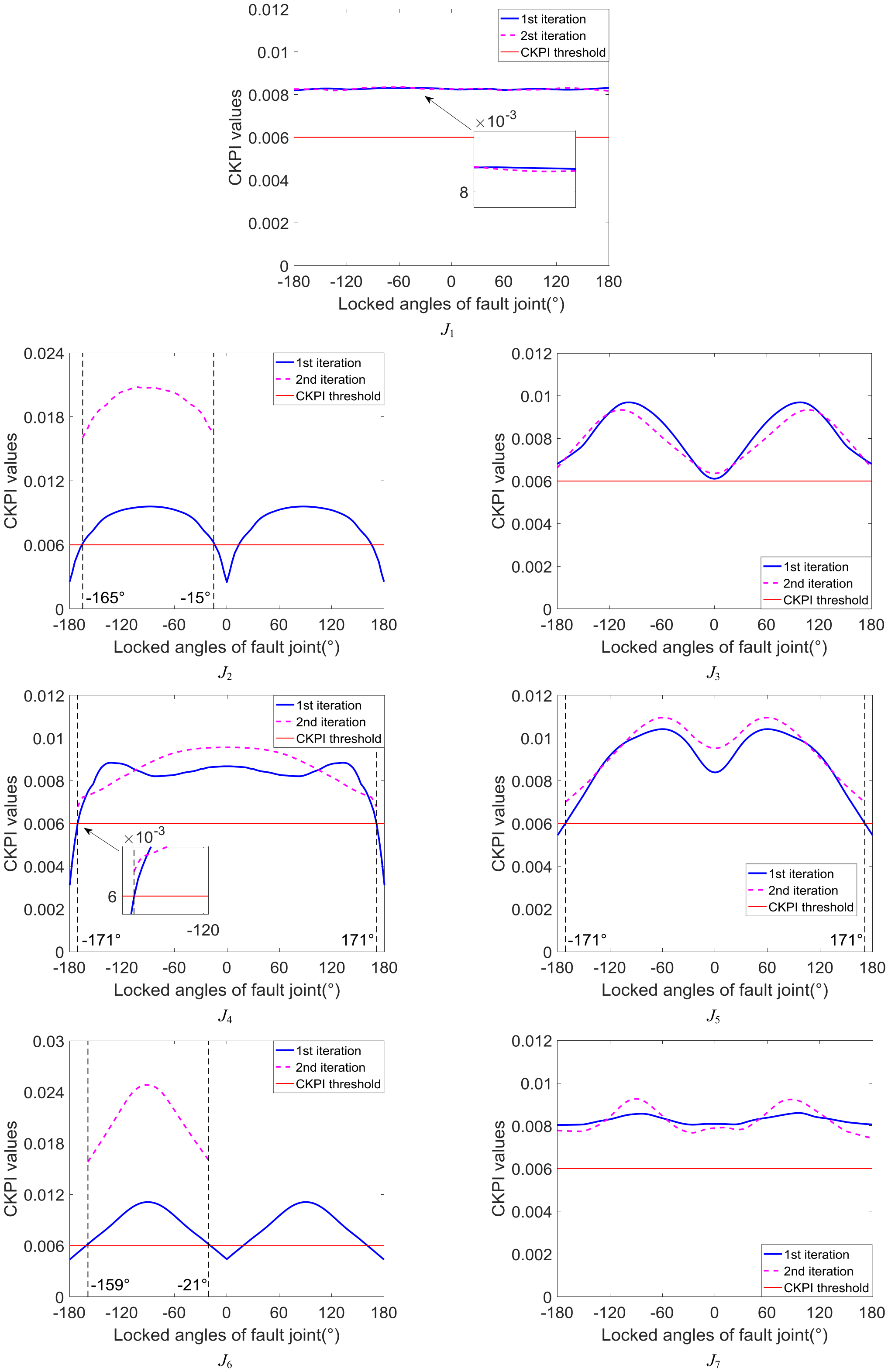

FIGURE 8. **Release the artificial limits of healthy joints and satisfy $CI_j \geq 0.006$.**

C. CKPI ANALYSIS

After completing the above simulation, we take J_4 as an example to analyze the kinematics performances of the manipulator when J_4 is locked at different angles. The changing curves of CKPI and the sub-indices (curves 1 to 6) included in CKPI of the manipulator are obtained as Fig. 10, which shows that the maximum values of reachable position workspace (curve 1), full orientation

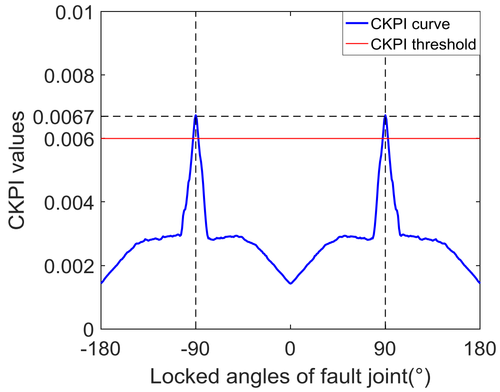

FIGURE 9. Solution result of the optimal locked angle of J_6 of the degraded manipulator.

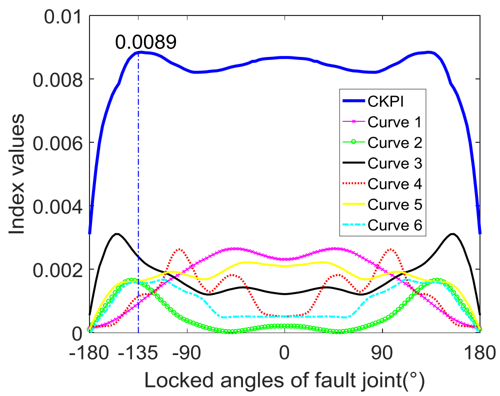

FIGURE 10. CKPI analysis of the manipulator with J_4 locked at different angles.

angle workspace (curve 2), global condition number (curve 3) and condition number fluctuation index (curve 4), the global minimum singular value (curve 5) and the minimum singular value fluctuation index (curve 6) are 0.0026, 0.0017, 0.0031, 0.0027, 0.0022 and 0.0018, respectively; and that the manipulator has the maximum CKPI value 0.0089 when J_4 is locked at $\pm 135°$. At this time, the values of the above sub-indices are 0.0009, 0.0016, 0.0024, 0.0007, 0.0017 and 0.0016, respectively. Although all the values of the sub-indices are not the maximum, most of them are closer to the maximum.

According to the above simulation results, we can know that the CKPI constructed in this paper can characterize the kinematics performances in both operation space and joint space simultaneously. When a space manipulator has the maximum CKPI value, its kinematics performances in both operation space and joint space is optimal as a whole. The method proposed in this paper for solving the artificial joint limits can effectively solve the coupling problem in the process of calculating the artificial joint limits. The coping strategy constructed in this paper can ensure that the kinematics performance of a space manipulator meets the requirements of the follow-up on-orbit operation tasks after multi-joint multi-type asynchronous failure. In summary, the above simulation results can verify the correctness and effectiveness of the coping strategy for multi-joint multi-type asynchronous failure of a space manipulator.

V. CONCLUTION

Aiming at solving the problem that the kinematics performance of a space manipulator cannot meet the requirements of the on-orbit operation tasks after multi-joint multi-type asynchronous failure, a coping strategy is proposed in this paper. Firstly, a CKPI is constructed based on the entropy method, which can be regarded as the criterion for solving the artificial joint limits and the optimal locked angle of a free-swinging fault joint. Secondly, for a space manipulator with joint locked failure, a prevention strategy of serious kinematics performance degradation is proposed based on the artificial joint limits; and through solving the optimal locked angle of fault free-swinging joint, a treatment strategy for joint free-swinging failure is developed. Finally, a coping strategy for multi-joint multi-type asynchronous failure of a space manipulator is constructed by synthesizing the above two strategies.

The main contributions of this paper are as follows: 1) the constructed CKPI can characterize the kinematics performances in both operation space and joint space simultaneously, so that the kinematics performances in both operation space and joint space of a space manipulator are optimal as a whole; 2) the method for solving the artificial joint limits based on the Newton-Raphson method is proposed, which can solve the coupling problem during solution and is universally suitable for all cases; 3) the proposed coping strategy can ensure that the kinematics performance of a space manipulator after multi-joint multi-type asynchronous failure still meets the requirements of the follow-up on-orbit operation tasks. In addition, the study results of this paper have reference value for the construction of the failure treatment strategy of other types of space manipulators. Moreover, the constructed CKPI and the proposed coping strategy can also be applied to other research fields of space manipulators, such as configuration design, task completion capability evaluation and trajectory optimization.

REFERENCES

[1] W. F. Xu, Y. She, and Y. S. Xu, "Analytical and semi-analytical inverse kinematics of SSRMS-type manipulators with single joint locked failure," *Acta Astronautica*, vol. 105, no. 1, pp. 201–217, 2014.

[2] J. D. English and A. A. Maciejewski, "Fault tolerance for kinematically redundant manipulators: Anticipating free-swinging joint failures," *IEEE Trans. Robot. Autom.*, vol. 14, no. 4, pp. 566–575, Aug. 1998.

[3] Y. She, W. F. Xu, H. Su, B. Liang, and H. K. Shi, "Fault-tolerant analysis and control of SSRMS-type manipulators with single-joint failure," *Acta Astronautica*, vol. 120, pp. 270–286, Mar./Apr. 2016.

[4] C. P. Pham, H. N. T. Phan, and P. J. From, "Comparison of mental and theoretical evaluations of remotely controlled mobile manipulators," *IFAC Proc. Vol.*, vol. 47, no. 3, pp. 326–331, 2014.

[5] B. Zhao, C. Li, D. Liu, and Y. Li, "Decentralized sliding mode observer based dual closed-loop fault tolerant control for reconfigurable manipulator against actuator failure," *PLoS ONE*, vol. 10, no. 7, p. e0129315, 2015.

[6] L. Chen, R. Patton, and S. Klinkhieo, "An LPV pole-placement approach to friction compensation as an FTC problem," *Int. J. Appl. Math. Comput. Sci.*, vol. 22, no. 1, pp. 149–160, 2012.

[7] F. Feng, L. Tang, J. Xu, H. Liu, and Y. Liu, "A review of the end-effector of large space manipulator with capabilities of misalignment tolerance and soft capture," *Sci. China-Technol. Sci.*, vol. 59, no. 11, pp. 1621–1638, 2016.
[8] X. Chen and S. Qin, "Kinematic modeling for a class of free-floating space robots," *IEEE Access*, vol. 5, pp. 12389–12403, 2017.
[9] Q. X. Jia, Y. Liu, G. Chen, H. X. Sun, and J. J. Peng, "Analysis of load-carrying capacity for redundant free-floating space manipulators in trajectory tracking task," *Math. Problems Eng.*, vol. 2014, Dec. 2014, Art. no. 125940.
[10] G. Genta and M. Dolci, "Robotic gripper for payload capture in low earth orbit," in *Proc. Int. Conf. Mech. Eng. Congr. Expo. (IMECE)*, Phoenix, AZ, USA, 2016, pp. 11–17.
[11] J. S. Guan, C.-M. Lin, G.-L. Ji, L.-W. Dian, and Y.-M. Zheng, "Robust adaptive tracking control for manipulators based on a TSK fuzzy cerebellar model articulation controller," *IEEE Access*, vol. 6, pp. 1670–1679, 2017.
[12] Z. Gao and D. Zhang, "Performance Analysis, mapping, and multiobjective optimization of a hybrid robotic machine tool," *IEEE Trans. Ind. Electron.*, vol. 62, no. 1, pp. 423–433, Jan. 2015.
[13] H. Y. Jin *et al.*, "Kinematics and cooperative control of a robotic spinal surgery system," *Robotica*, vol. 34, no. 1, pp. 1–17, 2016.
[14] Y. Ni, N. WU, X. Zhong, and B. Zhang, "Dimensional synthesis of a 3-DOF parallel manipulator with full circle rotation," *Chin. J. Mech. Eng.*, vol. 28, no. 4, pp. 830–840, 2015.
[15] K. Chen, J. Wang, W. Li, W. Li, and Y. Zhao, "Simulated feedback mechanism-based rotary kiln burning state cognition intelligence method," *IEEE Access*, vol. 5, pp. 4458–4469, 2017.
[16] J. Zhao and D. Peng, "Comprehensive evaluation of fault-tolerant properties of redundant robots," *Chin. J. Mech. Eng.*, vol. 21, no. 4, pp. 22–26, 2008.
[17] M. Goel, A. A. Maciejewski, V. Balakrishnan, and R. W. Proctor, "Failure tolerant teleoperation of a kinematically redundant manipulator: An experimental study," *IEEE Trans. Syst., Man, - Part A, Syst. Humans*, vol. 33, no. 6, pp. 758–765, Nov. 2003.
[18] R. C. Hoover, R. G. Roberts, and A. A. Maciejewski, "Implementation issues in identifying the failure-tolerant workspace boundaries of a kinematically redundant manipulator," in *Proc. IEEE/RSJ Int. Conf. Intell. Robots Syst.*, San Diego, CA, USA, Oct./Nov. 2007, pp. 3528–3533.
[19] C. L. Lewis and A. A. Maciejewski, "Fault tolerant operation of kinematically redundant manipulators for locked joint failures," *IEEE Trans. Robot. Autom.*, vol. 13, no. 4, pp. 622–629, Aug. 1997.
[20] R. G. Roberts, R. S. Jamisola, and A. A. Maciejewski, "Identifying the failure-tolerant workspace boundaries of a kinematically redundant manipulator," in *Proc. IEEE Int. Conf. Robot. Automation. (ICRA)*, Roma, Italy, Apr. 2007, pp. 4517–4523.
[21] S. F. M. Assal, "A novel planar parallel manipulator with high orientation capability for a hybrid machine tool: Kinematics, dimensional synthesis and performance evaluation," *Robotica*, vol. 35, no. 5, pp. 1031–1053, 2017.
[22] J. Li, J. F. Li, Z. Wu, and Q. X. Zhang, "Fault tolerance of redundant manipulators when multi-joint failed and its optimization," *Chin. J. Mech. Eng.*, vol. 38, no. 7, pp. 111–115, 2002.
[23] O. Y. Kanner, N. Rojas, L. U. Odhner, and A. M. Dollar, "Adaptive legged robots through exactly constrained and non-redundant design," *IEEE Access*, vol. 5, pp. 11131–11141, 2017.
[24] N. A. Khan, G. A. S. Sidhu, and F. F. Gao, "Optimizing combined emission economic dispatch for solar integrated power systems," *IEEE Access*, vol. 4, pp. 3340–3348, 2017.
[25] J. Nightingale and B. Goodwine, "An algorithm for stopping a class of underactuated nonlinear mechanical robotic systems," in *Proc. 21st Medit. Conf. Control Automat.*, Chania, Greece, Jun. 2013, pp. 531–536.
[26] J. D. English and A. A. Maciejewski, "Failure tolerance through active braking: A kinematic approach," *Int. J. Robot. Res.*, vol. 20, no. 20, pp. 287–299, 2007.
[27] X. Yang, H. Wang, C. Zhang, and K. Chen, "A method for mapping the boundaries of collision-free reachable workspaces," *Mechanism Mach. Theory*, vol. 45, no. 7, pp. 1024–1033, 2010.
[28] K. K. Aydin, "Implications of faults in manipulator joints on the workspace," in *Proc. 8th Medit. Electrotechn. Conf. (MELECON)*, Bari, Italy, May 1996, pp. 197–200.
[29] M. Bergerman and Y. S. Xu, "Dexterity of underactuated manipulators," in *Proc. 8th Int. Conf. Adv. Robot. (ICAR)*, Monterey, CA, USA, Jul. 1997, pp. 719–724.
[30] F. Aghili and F. Aghili, "Failure detection and isolation in robotic manipulators using joint torque sensors," *Robotica*, vol. 28, no. 4, pp. 549–561, 2010.
[31] Y. Wang, S. Jiang, B. Chen, and H. Wu, "Trajectory tracking control of underwater vehicle-manipulator system using discrete time delay estimation," *IEEE Access*, vol. 5, pp. 7435–7443, 2017.
[32] R. C. Hoover, R. G. Roberts, A. A. Maciejewski, P. S. Naik, and K. M. Ben-Gharbia, "Designing a failure-tolerant workspace for kinematically redundant robots," *IEEE Trans. Autom. Sci. Eng.*, vol. 12, no. 4, pp. 1421–1432, Oct. 2015.
[33] M. Isaksson, K. Marlow, A. Maciejewski, and A. Eriksson, "Novel fault-tolerance indices for redundantly actuated parallel robots," *J. Mech. Des.*, vol. 139, no. 4, p. 042301, 2017.
[34] X. Zhang and J. Liu, "Autonomous trajectory planner for space telerobots capturing space debris under the teleprogramming framework," *Adv. Mech. Eng.*, vol. 9, no. 9, pp. 1–13, 2017.

QINGXUAN JIA received the B.S. and M.S. degrees in mechanical engineering from the Shandong University of Technology, Shandong, China, in 1988 and 1991, respectively, and the Ph.D. degree in electromechanical engineering and automation from the Beijing University of Aeronautics and Astronautics, Beijing, China, in 2005.

He is currently a Professor with the School of Automation, Beijing University of Posts and Telecommunications. His research topics include space robotics, virtual reality technology, and pattern recognition.

XUAN WANG received the B.S. degree in mechanical engineering and automation from the Beijing University of Posts and Telecommunications, Beijing, China, in 2016, where he is currently pursuing the M.S. degree in mechatronic engineering.

His research topics include space robotics, fault tolerance, and kinematics analysis.

GANG CHEN received the B.S. degree in mechanical design-manufacture and automation from the Beijing Institute of Petrochemical Technology, Beijing, China, in 2004, and the Ph.D. degree in mechatronic engineering from the Beijing University of Posts and Telecommunications, Beijing, in 2011.

He is currently an Associate Professor with the School of Automation, Beijing University of Posts and Telecommunications. His research topics include space robotics, and motion planning and control method.

BONAN YUAN received the B.S. degree in mechanical engineering and automation from the Beijing University of Posts and Telecommunications, Beijing, China, in 2015, where he is currently pursuing the Ph.D. degree in mechatronic engineering.

His research topics include space robotics, failure detection and recovery, and robot control method.

YINGZHUO FU received the B.S. degree in mechanical engineering and automation from the Beijing University of Posts and Telecommunications, Beijing, China, in 2017, where he is currently pursuing the Ph.D. degree in mechanical engineering.

His research topics include space robotics, fault tolerance, and robot control method.